

Optimal Multi-Debris Mission Planning in LEO: A Deep Reinforcement Learning Approach with Co-Elliptic Transfers and Refueling

Agni Bandyopadhyay* Günther Waxenegger-Wilfing**

* *Department of Computer Science, Julius-Maximilians-Universität Würzburg, Germany (e-mail: agni.bandyopadhyay@uni-wuerzburg.de)*

** *Department of Computer Science, Julius-Maximilians-Universität Würzburg, Germany (e-mail: guenther.waxenegger@uni-wuerzburg.de)*

Abstract: This paper addresses the challenge of multi-target active debris removal (ADR) in Low Earth Orbit (LEO) by introducing a unified co-elliptic maneuver framework that combines Hohmann transfers, safety ellipse proximity operations, and explicit refueling logic. We benchmark three distinct planning algorithms—Greedy heuristic, Monte Carlo Tree Search (MCTS), and deep reinforcement learning (RL) using Masked Proximal Policy Optimization (PPO)—within a realistic orbital simulation environment featuring randomized debris fields, keep-out zones, and ΔV constraints. Experimental results over 100 test scenarios demonstrate that Masked PPO achieves superior mission efficiency and computational performance, visiting up to twice as many debris as Greedy and significantly outperforming MCTS in runtime. These findings underscore the promise of modern RL methods for scalable, safe, and resource-efficient space mission planning, paving the way for future advancements in ADR autonomy.

1. INTRODUCTION

The proliferation of space debris in Low Earth Orbit (LEO) has become a growing concern for the global space community, threatening both operational spacecraft and the long-term sustainability of space activities European Space Agency (2023); NASA (2008). Over 36,000 trackable debris objects larger than 10 cm and millions of smaller fragments are now in orbit, resulting from collisions, break-ups, and routine operations European Space Agency (2023); Kessler and Cour-Palais (1978). This increasing population, if left unmanaged, poses the risk of the so-called “Kessler Syndrome”—a cascading effect of collisions generating ever more debris Kessler and Cour-Palais (1978); Stenger (2002).

Active Debris Removal (ADR) is now widely recognized as an essential measure to ensure the safety and sustainability of space operations Bonnal et al. (2013). ADR missions typically involve a chaser spacecraft executing a sequence of autonomous rendezvous maneuvers to capture and de-orbit multiple debris targets within stringent fuel and time constraints Federici and Colasurdo (2019). Efficient planning of the visitation sequence is crucial to maximize mission effectiveness while minimizing resources.

Traditionally, the multi-debris rendezvous problem has been approached as a variant of the Traveling Salesman Problem (TSP) Gutin and Karapetyan (2008); Federici and Colasurdo (2019), using classical heuristics such as greedy search, genetic algorithms, or simulated annealing Corman et al. (2009a); Halim and Ismail (2019). While

these techniques are computationally efficient and well-studied, they often fail to capture the full complexity of space mission constraints, such as refueling, keep-out zones, and dynamic collision avoidance.

Recent years have witnessed a surge in learning-based approaches for trajectory optimization and space mission planning. Deep reinforcement learning (RL), in particular, offers the ability to synthesize adaptive, scalable policies for high-dimensional, uncertain environments Mazyavkina et al. (2021); Sutton and Barto (2018); Stephenson et al. (2025); Dunlap et al. (2024). Notably, RL agents have demonstrated strong performance in sequencing debris rendezvous operations Bandyopadhyay and Waxenegger-Wilfing (2024, 2025), often outperforming popular traditional heuristics in both solution quality and computational speed.

In our previous work, Bandyopadhyay and Waxenegger-Wilfing (2024), we introduced a policy gradient Reinforcement Learning (RL) agent for sequencing multi-debris visits, achieving a significant reduction in total rendezvous time compared to standard heuristics. We subsequently extended this framework to incorporate refueling and dynamic collision avoidance zones Bandyopadhyay and Waxenegger-Wilfing (2025), moving closer to the requirements of real-world ADR missions.

This paper advances the state of the art by introducing a unified co-elliptic maneuver framework that seamlessly integrates Hohmann transfers, safety ellipse detours Barbee et al. (2011), and explicit refueling logic.

To rigorously evaluate our approach, we benchmark our trained reinforcement learning agent against established heuristic baselines, namely Monte Carlo Tree Search (MCTS) Browne et al. (2012) and a classical Greedy algorithm Cormen et al. (2009b). The mission planning challenge addressed in this work is inherently twofold: efficiency can be improved either through optimizing the underlying trajectory planning or by enhancing the decision-making strategy. In this study, we seek to deepen our understanding of the problem by making targeted advancements in both aspects.

2. RELATED WORK

Multi-target trajectory optimization for active debris removal (ADR) has evolved from early combinatorial heuristics—such as the beam search, and greedy algorithms—to data-driven and reinforcement learning (RL) frameworks. Classical methods focused on minimizing cumulative ΔV or total transfer time across multiple targets Letizia et al. (2017); Petit et al. (2012); Herrmann and Schaub (2022). Additionally, we incorporate real-world constraints—namely fuel availability and overall mission duration—into the framework.

A fundamental maneuver for orbital rendezvous is the Hohmann transfer, which computes the minimum-energy transfer between two coplanar circular orbits Hohmann (1925); Curtis (2013). However, when visiting a sequence of debris objects distributed along similar orbits, performing a standard Hohmann transfer between each pair can lead to excessive and inefficient trajectory changes. To address this, *co-elliptic* Hohmann transfers are used: the chaser spacecraft is placed into an intermediate co-elliptic orbit that shares the target’s apogee or perigee and thus gradually phases around the Earth to rendezvous with the debris Vallado (2001). This strategy allows for more efficient multi-target rendezvous when the debris are clustered in similar orbital bands, reducing both ΔV and mission time compared to a sequence of isolated transfers. It also significantly improves and quickens the phasing maneuvers and also leaves room for quick changes if necessary. Figure 1 provides an overview of this co-elliptic maneuver sequence, highlighting the initial and target orbits, transfer maneuvers, and the terminal safety ellipse approach.

Another critical aspect of proximity operations is the terminal approach and safety management. Standard Hohmann transfers do not address the need for controlled, precise, and safe approaches to non-cooperative targets like space debris. To mitigate the risk of collision during close-approach, recent frameworks integrate a *safety ellipse maneuver* as proposed in Barbee et al. (2011), which prescribes an elliptical slow approach to the target. This maneuver enables the chaser to approach within a predefined miss distance, maintaining both safety and controllability in the final rendezvous phase. Such maneuvers are widely adopted in operational spacecraft proximity operations to enforce strict safety requirements and provide margins against navigation errors and unmodeled dynamics Alonso et al. (2009). Figure 2 illustrates a

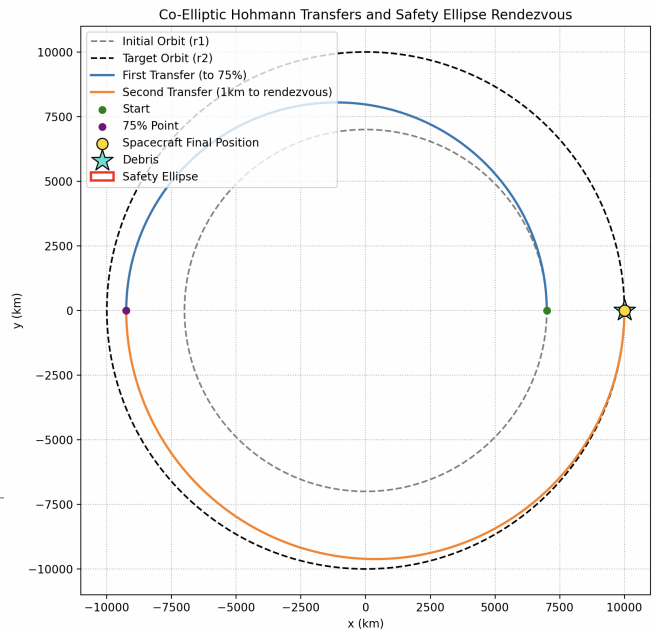


Fig. 1. Overview of the co-elliptic Hohmann transfer sequence, showing the initial and target orbits, transfer maneuvers, and the terminal safety ellipse maneuver at rendezvous.

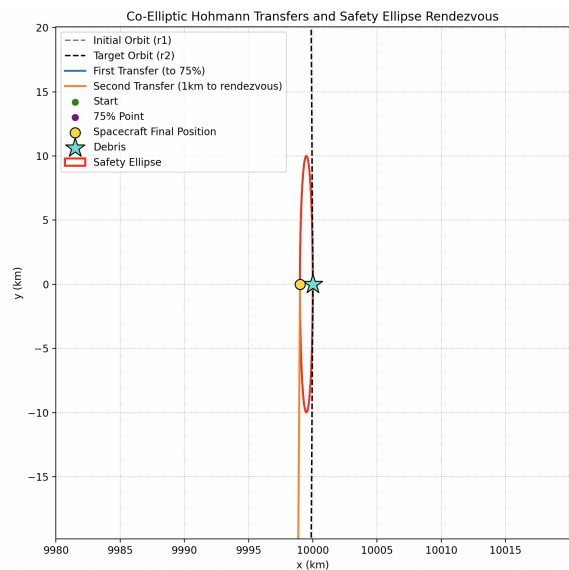


Fig. 2. Zoomed-in view of the terminal approach phase, highlighting the safety ellipse maneuver for controlled and safe rendezvous with the target debris.

zoomed-in view of the terminal approach phase, showing the chaser spacecraft and debris within the safety ellipse during final approach.

Learning-based methods provide additional flexibility in this setting. Nevertheless, integrating co-elliptic transfers and safety ellipse maneuvers into sequential multi-target planning for ADR remains a challenging problem for both traditional and RL-based systems.

3. MISSION MODEL

3.1 Operational Scenario

We consider an autonomous service spacecraft tasked with maximizing the number of debris objects visited and actively serviced within a fixed low Earth orbit (LEO) mission window. At the start of each episode, the chaser is initialized docked at a refueling station in a circular orbit of 700 km altitude, representing a typical LEO servicing platform. The environment generates a population of $N = 50$ debris targets per episode, each with randomly sampled altitudes, inclinations, and other orbital elements, reflecting the diversity and spatial spread of real-world LEO debris fields.

The agent operates in discrete decision steps. At each step, it may select a debris object for rendezvous or opt to return to the refueling station. Each debris visitation comprises a transfer maneuver, a brief period of station-keeping (e.g., one orbital period) to simulate servicing or data collection, and a subsequent decision to continue the mission or to refuel. Debris objects already visited are flagged and cannot be re-selected within the same episode.

3.2 Transfer and Maneuver Model

Inter-debris transfers are executed using a co-elliptic Hohmann transfer sequence to ensure realistic and efficient phasing and rendezvous operations. Specifically, for each target selection:

- (1) The chaser initiates a maneuver to raise or lower its orbit to a co-elliptic trajectory that matches the altitude of the target debris, optimizing both transfer time and ΔV .
- (2) After appropriate phasing, a final burn circularizes the chaser’s orbit to precisely match the debris’ position, enabling rendezvous.

The transfer sequence accounts for orbital inclination changes as needed, and ensures that all maneuvers adhere to the constraints of orbital mechanics.

The first Hohmann transfer is conducted to cover 75 percent of the distance between the chaser and the debris. Then the next Hohmann transfer brings the chaser within 1 km of the target after which it embarks on the safety ellipse maneuver to approach the target. The safety ellipse provides both control and accuracy in proximity operations.

3.3 Refueling and ΔV Budgeting

Propellant consumption is modeled directly via cumulative ΔV expended by the chaser, treating ΔV as a proxy for fuel usage. The agent may return to the refueling station at any time after successfully visiting at least one debris object. Upon docking, the agent’s available ΔV budget is fully replenished; however, this incurs additional time and maneuvering penalties associated with the round-trip. This refueling logic encourages efficient path planning and penalizes excessive refueling cycles.

3.4 Mission Constraints

The following operational constraints are strictly enforced throughout each episode:

- **ΔV Limit:** The chaser is initialized with a fixed ΔV budget (e.g., 3 km/s), which governs the maximum total velocity change available for all maneuvers before requiring refueling.
- **Mission Duration:** Each mission is bounded by a maximum allowed duration, such as 7 days, after which the episode terminates regardless of the number of debris visited.
- **Population Size:** Each episode contains a fixed set of $N = 50$ debris objects, with random orbital parameters to ensure diversity and robustness in planning strategies.

This operational scenario and maneuver model capture the critical challenges of multi-target rendezvous in cluttered LEO environments, while providing a flexible framework for benchmarking planning algorithms under realistic resource and safety constraints.

4. PLANNING ALGORITHMS

This work benchmarks three distinct planning approaches for multi-target debris removal: a classical greedy heuristic, a Monte Carlo Tree Search (MCTS) planner, and a reinforcement learning (RL) agent. All algorithms operate under the same mission constraints and orbital mechanics, as described in Section 2.

4.1 Greedy Heuristic

The greedy algorithm selects, at each decision step, the next unvisited debris object d^* that minimizes the incremental cost, defined as a weighted sum of ΔV and transfer time:

$$d^* = \arg \min_{d \in \mathcal{D}_{\text{unvisited}}} [\alpha \Delta V_{\text{curr} \rightarrow d} + \beta T_{\text{curr} \rightarrow d}] \quad (1)$$

where $\mathcal{D}_{\text{unvisited}}$ is the set of all remaining debris, $\Delta V_{\text{curr} \rightarrow d}$ is the velocity cost, $T_{\text{curr} \rightarrow d}$ is transfer time, and α, β are normalization or weighting coefficients (typically $\alpha = 1, \beta = 0$ for pure ΔV minimization). The greedy agent triggers a refueling maneuver if no reachable debris remains within the current ΔV and time budgets. This approach is inherently myopic, optimizing for immediate reward rather than long-term mission success (Cormen et al. (2009b)).

4.2 Monte Carlo Tree Search (MCTS)

MCTS Browne et al. (2012) constructs a search tree from the current mission state, recursively expanding child nodes corresponding to feasible debris selections or refueling decisions. At each node, the Upper Confidence Bound (UCB) formula guides the balance between exploration and exploitation:

$$\text{UCB}_i = Q_i + C \sqrt{\frac{\ln N}{n_i}} \quad (2)$$

where Q_i is the mean simulated return for child i , n_i is the number of times child i has been visited, N is the total number of simulations from the parent node, and C is the exploration constant. Leaf nodes are expanded using random rollouts to estimate the cumulative reward (e.g., total debris visited), and backpropagation updates values up the tree. The action selected is the child of the root with the highest visit count or value after a fixed number of simulations.

4.3 Reinforcement Learning Agent

Proximal Policy Optimization (PPO) Schulman et al. (2017) is a policy gradient algorithm that stabilizes training by constraining policy updates through a clipping mechanism, and in this work we employ a specialized variant, Masked PPO, which extends PPO by incorporating action masks to exclude infeasible actions from the policy distribution Tang et al. (2020); Huang and Ontaño (2022). This was used to train a RL agent within a custom OpenAI Gym environment that simulates the ADR mission Bandyopadhyay and Waxenegger-Wilfing (2024, 2025). The observation vector \mathbf{o}_t at timestep t includes:

- A binary mask of visited debris
- Remaining ΔV budget
- Remaining mission time
- Current chaser orbital parameters (all six Keplerian elements)
- Orbital parameters of all debris (all six Keplerian elements)

The discrete action space \mathcal{A}_t consists of all debris plus the option to refuel at the station. We used action masking to mask the visited debris from the action space over time so that only new debris can be visited over time. The reward function is defined as:

$$r_t = \begin{cases} +1 & \text{for each successful debris rendezvous} \\ 0 & \text{for refueling or detour actions} \\ -1 & \text{for early termination or constraint violation} \end{cases} \quad (3)$$

If the agent runs out of fuel or time the episode is terminated and this makes the agent learn over time to prioritize visiting new debris. Training is performed with randomly generated debris fields to encourage generalization and robustness across mission scenarios.

4.4 Unified Evaluation Framework

All planning algorithms are evaluated within a unified simulation framework, ensuring consistent orbital dynamics, mission constraints, and environment interactions. Key performance metrics include:

- **Debris Visited:** Total number of distinct debris serviced per episode.
- **Total Computational time:** Total time taken by the algorithm to plan the mission.

This evaluation protocol allows for direct, fair comparison of solution quality, mission efficiency, and computational tractability across the three planning paradigms.

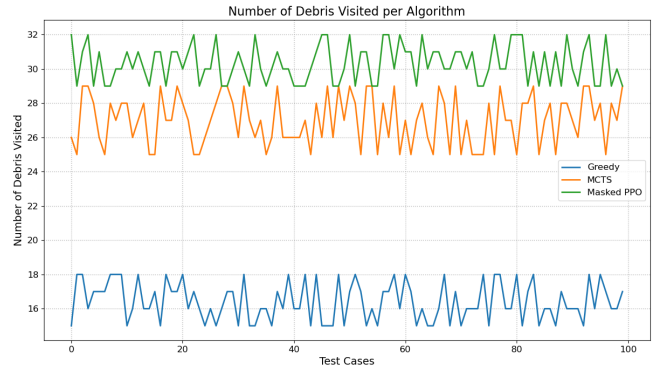


Fig. 3. Number of debris objects visited per episode by each algorithm across 100 randomized test cases.

5. RESULTS AND DISCUSSION

The performance of the three planning algorithms—Greedy heuristic, Monte Carlo Tree Search (MCTS), and Masked Proximal Policy Optimization (PPO)—was evaluated over 100 randomized test cases. The primary metrics of interest are (i) the total number of debris objects successfully visited per episode and (ii) the computation time required for each planner, as shown in Figures 3 and 4.

5.1 Debris Removal Efficiency

Figure 3 shows the number of debris visited per test case for each algorithm. The Greedy heuristic consistently achieves the lowest performance, visiting between 15 and 18 debris objects per episode, due to its myopic decision-making and lack of long-term trajectory optimization. MCTS significantly improves upon this baseline, with visit counts ranging from 25 to 29 debris per episode. The improved performance of MCTS is attributed to its ability to simulate future trajectories and optimize cumulative reward, at the expense of higher computational complexity.

The Masked PPO agent outperforms both baselines, visiting between 29 and 32 debris objects per test case. Its ability to generalize across randomized debris fields and to learn long-term reward maximization enables it to consistently select more efficient multi-target rendezvous sequences. The RL agent’s performance demonstrates the value of learning-based strategies in high-dimensional, sequential decision-making environments, where both operational constraints and future rewards must be balanced.

5.2 Computation Time

Computation time for each algorithm is shown in Figure 4 on a logarithmic scale. The Greedy and Masked PPO planners both exhibit extremely fast inference, typically solving each episode in 1–2 seconds on average. In contrast, MCTS is orders of magnitude slower, with episode computation times ranging from approximately 1,000 to 10,000 seconds, due to the need for extensive tree expansion and rollouts at each decision point. This substantial

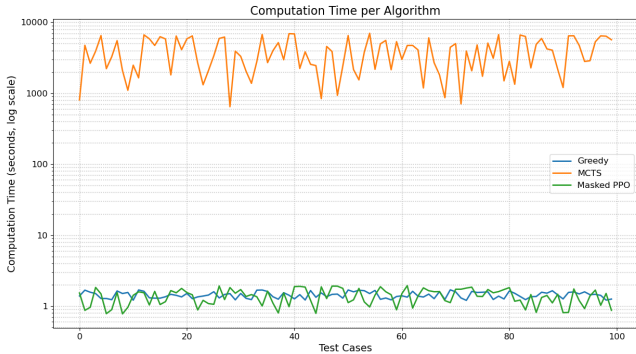


Fig. 4. Computation time (log scale) for each algorithm per test case. Masked PPO and Greedy achieve fast runtimes, while MCTS is orders of magnitude slower.

difference highlights a key practical limitation of search-based methods for large-scale, real-time mission planning.

5.3 Discussion

The results clearly indicate that Masked PPO achieves the best balance between solution quality and computational efficiency. While MCTS is capable of generating high-quality plans, its prohibitive runtime makes it impractical for on-board or real-time applications. The Greedy agent, though computationally efficient, is severely limited by its short-sightedness, missing many reachable debris objects in complex scenarios.

The Masked PPO agent demonstrates strong generalization to randomized debris fields and robustly respects mission constraints, including refueling logic. These findings support the growing consensus that deep reinforcement learning, when combined with accurate orbital dynamics simulation and carefully designed action masking, can enable scalable and reliable mission planning for active debris removal and similar sequential decision-making problems in space operations.

6. CONCLUSION

This paper presented a unified co-elliptic maneuver framework for multi-target active debris removal (ADR), integrating Hohmann transfers, safety ellipse maneuvers, and explicit refueling logic within a realistic orbital environment. We systematically tested our policy against traditional planning heuristics like—Greedy heuristic and Monte Carlo Tree Search (MCTS)—under identical mission constraints and randomized debris scenarios.

Our results demonstrate that the Masked PPO agent achieves the best overall trade-off between mission efficiency and computational feasibility, consistently outperforming traditional search-based and heuristic methods in both solution quality and runtime. While MCTS approaches near-optimal visitation counts, its high computational cost limits its practicality for real-time or on-board implementation. The Greedy agent offers fast but suboptimal solutions, frequently missing reachable debris due to its myopic strategy.

These findings highlight the potential of modern RL approaches for complex, high-dimensional space mission planning tasks, where long-term objectives, operational safety, and computational efficiency must all be balanced. Future work will explore the integration of more detailed dynamical models, transfer learning for adaptation to changing debris fields, and further onboard validation to support next-generation ADR missions to make the simulation more realistic and practical.

APPENDIX

A. Mission Parameters

- **Initial Orbit and Refuelling Orbit:** 700 km circular orbit, 96° inclination.
- **Target Debris:** 50 objects uniformly sampled per episode randomly between 700 and 800 km altitude.
- **Fuel Capacity:** Normalized to 1.0 at start; reset to full on refuel calculated with reference to the maximum dV.
- **Max dV:** Set at 3 km/s.
- **Maximum Episode Duration:** Each test case has a duration of 7 days within which the agent has to visit as many debris as possible.
- **Episode Termination:** All debris visited, fuel exhausted, running out of time or invalid action.
- **Test Case Variation:** Each test case has generates 50 random debris. Each test case is tested for 10 iterations with each strategy as the collisions are completely randomized per iteration.
- **Assumptions:** We assume no effect of the J2 perturbations.

B. Reinforcement Learning Hyperparameters

The hyperparameters were tuned as per our previous work.

- **Algorithm:** Proximal Policy Optimization (Masked PPO).
- **Learning Rate:** 5×10^{-6} .
- **Training Steps:** 10 million.
- **Batch Size:** 2048.
- **Discount Factor (γ):** 0.99.
- **Clipping Parameter (ϵ):** 0.2.
- **Action Masking:** Enabled (invalid actions set to $-\infty$ logits).
- **Policy Network:** Multilayer Perceptron (MLP) with two hidden layers, 256 neurons each, \tanh activation.
- **Framework:** Stable-Baselines3 + Poliastro.

C. Plain MCTS and Greedy Configuration

- **MCTS Algorithm:** Plain Monte Carlo Tree Search using UCT.
- **Exploration Constant:** $c_{uct} = 1.5$.
- **Simulations per Step:** 200.
- **Rollout Depth:** 15.
- **Greedy Algorithm:** The standard greedy algorithm is used and it chooses the rendezvous with the lowest dv.

E. Environment Settings

- **Astrodynamics Libraries:** Poliastro, Astropy.
- **Hardware:** MacBook Pro M1 Max, 64 GB RAM, Python 3.11.

REFERENCES

- Alonso, R., Aznar, F., and Pernas, M. (2009). Collision avoidance maneuvers for proximity operations in autonomous rendezvous missions. *Acta Astronautica*, 65(9-10), 1537–1548.
- Bandyopadhyay, A. and Waxenegger-Wilfing, G. (2024). Revisiting space mission planning: A reinforcement learning-guided approach for multi-debris rendezvous. In *2024 International Conference on Space Robotics (iSpaRo)*, 104–110. doi:10.1109/iSpaRo60631.2024.10687704.
- Bandyopadhyay, A. and Waxenegger-Wilfing, W. (2025). Optimizing mission planning for multi-debris rendezvous using reinforcement learning with refueling and adaptive collision avoidance. In *Proc. IAA Small Satellite Symposium Berlin 2025 (in publication)*.
- Barbee, B.W., Carpenter, J.R., Heatwole, S., Markley, F.L., Moreau, M.C., Naasz, B.J., and Eepoel, J.V. (2011). A guidance and navigation strategy for rendezvous and proximity operations with a noncooperative spacecraft in geosynchronous orbit. *The Journal of the Astronautical Sciences*, 58, 389–408. doi:10.1007/bf03321176.
- Bonnal, C., Ruault, J.M., and Desjean, M.C. (2013). Active debris removal: Recent progress and current trends. *Acta Astronautica*, 85, 51–60. doi:10.1016/j.actaastro.2012.11.009.
- Browne, C.B., Powley, E., Whitehouse, D., Lucas, S.M., Cowling, P.I., Rohlfshagen, P., Tavener, S., Perez, D., Samothrakis, S., and Colton, S. (2012). A survey of monte carlo tree search methods. *IEEE Transactions on Computational Intelligence and AI in Games*, 4(1), 1–43.
- Cormen, T.H., Leiserson, C.E., Rivest, R.L., and Stein, C. (2009a). *Introduction to Algorithms*. MIT Press, 3rd edition.
- Cormen, T.H., Leiserson, C.E., Rivest, R.L., and Stein, C. (2009b). *Introduction to Algorithms*. MIT press.
- Curtis, H.D. (2013). *Orbital Mechanics for Engineering Students*. Elsevier, 3rd edition.
- Dunlap, K., Hamilton, N., and Hobbs, K.L. (2024). Deep reinforcement learning for scalable multi-agent spacecraft inspection. doi:10.48550/arXiv.2412.10530. URL <https://arxiv.org/abs/2412.10530>. ArXiv:2412.10530.
- European Space Agency (2023). Space debris by the numbers. URL https://www.esa.int/Safety_Security/Space_Debris/Space_debris_by_the_numbers. ESA Space Debris Office, ESOC, Darmstadt, Germany.
- Federici, A. and Colasurdo, G. (2019). A time-dependent tsp formulation for the design of an active debris removal mission using simulated annealing. *Astrodynamics*. URL <https://arxiv.org/abs/1909.10427>. ArXiv:1909.10427.
- Gutin, G. and Karapetyan, D. (2008). Greedy like algorithms for the traveling salesman and multidimensional assignment problems. In *Greedy Algorithms: Theory and Applications*, 291–304. Springer.
- Halim, A.H. and Ismail, I. (2019). Combinatorial optimization: Comparison of heuristic algorithms in travelling salesman problem. *Archives of Computational Methods in Engineering*, 26, 367–380.
- Herrmann, A. and Schaub, H. (2022). Monte carlo tree search methods for the earth-observing satellite scheduling problem. *Journal of Aerospace Information Systems*, 19, 70–82. doi:10.2514/1.i010992.
- Hohmann, W. (1925). Die erreichbarkeit der himmelskörper. *Darmstadt: Oldenbourg*.
- Huang, S. and Ontañón, S. (2022). A closer look at invalid action masking in policy gradient algorithms. In *Proceedings of the International FLAIRS Conference*, volume 35. doi:10.32473/flairs.v35i.130584.
- Kessler, D.J. and Cour-Palais, B.G. (1978). Collision frequency of artificial satellites: The creation of a debris belt. *Journal of Geophysical Research*, 83(A6), 2637–2646. doi:10.1029/JA083iA06p02637.
- Letizia, F., Colombo, C., and Lewis, H.G. (2017). Optimal mission planning for multiple space debris removal. *Journal of Guidance, Control, and Dynamics*, 40(2), 450–464.
- Mazyavkina, N., Sviridov, S., Ivanov, S., and Burnaev, E. (2021). Reinforcement learning for combinatorial optimization: A survey. *Computers & Operations Research*, 134, 105400. doi:10.1016/j.cor.2021.105400.
- NASA (2008). Handbook for limiting orbital debris. Technical Report NASA-HDBK-8719.14, NASA. URL https://orbitaldebris.jsc.nasa.gov/library/usg_od_handbook.pdf.
- Petit, N., Brisset, P., and Bensalah, D. (2012). Multiple space debris collecting missions: Combinatorial optimization. *Journal of Guidance, Control, and Dynamics*, 35(5), 1577–1589.
- Schulman, J., Wolski, F., Dhariwal, P., Radford, A., and Klimov, O. (2017). Proximal policy optimization algorithms. In *arXiv preprint arXiv:1707.06347*.
- Stenger, R. (2002). Scientist: Space weapons pose debris threat. URL <https://www.cnn.com/2002/TECH/space/05/02/space.debris/index.html>. CNN.com, May 3, 2002.
- Stephenson, M., Prats, D.H., and Schaub, H. (2025). Autonomous satellite inspection in low earth orbit with optimization-based safety guarantees. In *International Workshop on Planning & Scheduling for Space*. Toulouse, France.
- Sutton, R.S. and Barto, A.G. (2018). *Reinforcement Learning: An Introduction*. MIT Press, 2nd edition. URL <http://incompleteideas.net/book/the-book-2nd.html>.
- Tang, C.Y., Liu, C.H., Chen, W.K., and You, S.D. (2020). Implementing action mask in proximal policy optimization (ppo) algorithm. *ICT Express*, 6(3), 200–203. doi:10.1016/j.ict.2020.05.003.
- Vallado, D.A. (2001). *Fundamentals of Astrodynamics and Applications*. Microcosm Press, 2nd edition.